LARGE DEPLOYABLE ANTENNA REFLECTOR TRIMMING MECHANISM (LDA-RTM)

Miguel Domingo , Jorge Vázquez

SENER Ingeniería y Sistemas, S.A.
Avda. Zugazarte 56, 48930 Getxo, Vizcaya, Spain
Tel: +34 94 481 7500 / Fax: +34 94 481 7603 / E-mail: miguel.domingo@sener.es

ABSTRACT

Future projects dealing with radars or telecommunications require deployable antennas. ESA Contract no. 15230 for the "Development of Large Deployable Antenna Reflector for Advanced Mobile Communication" has the objective of developing this critical technology in Europe for the commercial market.
The Reflector Trimming Mechanism (RTM) allows the fine adjustment of the huge Reflector Dish (12 meters projected aperture diameter) in such a way to recover the mispointing induced by all sources inclusive of the S/C, the Antenna Arm, the feed and the Reflector.
The RTM design is modular and allows its implementation in different reflector types and dimensions changing the distance between movable and fixed points and the lateral stiffener.
In each linear actuator, it is implemented a device which is able to decouple the top and the bottom part. This is required because of imposed displacements of the interfaces during launch. The decoupling device is latched before starting normal operating condition. It is actuated with the same stepper motor used for trimming.
The RTM has been designed to be operated with the electronic box already developed for moving the Antenna Pointing Mechanism in Hispasat 1-C.

1. INTRODUCTION

The Reflector Trimming Mechanism (RTM) is an assembly included in the Large Deployable Antenna (LDA) to perform the fine adjustment of the Reflector Dish.
More specific functions of the RTM are:

- to withstand launch environmental conditions;
- to hold the reflector in position when unpowered;
- to perform the two axes trimming operation;

The operation modes of the RTM are:

· Launch mode: No power is available. The RTM rests between the Large Deployable Reflector (LDR) and the Arm in the "zero" angular position. In this mode the RTM should withstand, without degradation, launch environmental loads. The axial decoupling device of the linear actuator is unlatched, so there can be movements between two interfaces of the linear actuator transmitting very little forces to the actuator.

· Deployment mode: No power is available. The RTM is in the same "zero" position of the previous mode and is able to withstand LDA deployment induced loads without degradation and maintaining the reflector in position. The axial decoupling device is latched, so it can transmit the forces and provide stiffness to the RTM.

· Holding mode: No power is available. The RTM can be in any angular position within its operational range and is able to withstand AOCS induced loads without degradation and holding the reflector in position.

· Trimming mode: Power is available. The RTM is able to align the LDR within its angular range upon external command under nominal orbit environmental conditions.

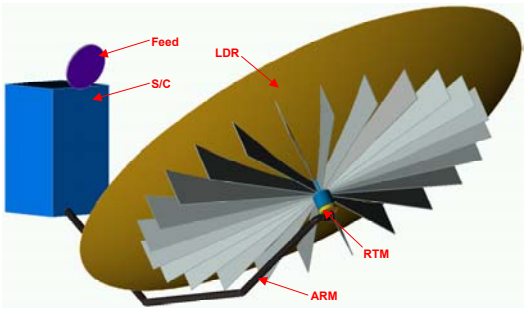

Figure 1, RTM position in the LDA

The conceptual design of the two axis trimming mechanism consists of three elements connecting the LDR and the ADB (Arm Hinge Deployment & Blocking Mechanism). One of the elements is a fixed support ending in a spherical joint. The other two elements are linear actuators with a flexible gimbal at one end and a spherical joint at the other end (same end where the fixed element has its spherical joint) and a elastic lateral stiffener. Next figure shows the symbolic kinematics of the concept and the QM.

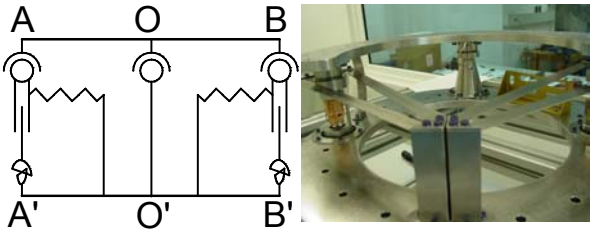

Figure 2, Trimming concept and Qualification Model

The fixed element constrains three translation degree of freedom (dof), leaving free the three rotational dof around the spherical joint. Each linear actuator, when fixed in length, constrains one dof (distance between gimbal and spherical joints). The remaining degree of freedom at RTM level, which is the rotation around the vertical axis passing through the fixed spherical joint, is constrained by means of the combination of the two elastic lateral stiffeners, which allow the vertical displacement but are very stiff in the direction of the attachment point in the dof they constrain.
The three spherical joints are arranged in an isosceles square triangle. This configuration presents two advantages: it provides axes orthogonality and similar positioning algorithms for both trimming axes. Besides, due to the reduced trimming range, the rotation of each axis is practically linear with respect to the linear actuator displacement. The trimming operation is performed varying the length of the linear actuators.

RTM main characteristics

The RTM is able to position the fully deployed Reflector Dish between a range of ±1.5° on each orthogonal axis.
The RTM resolution is driven by the following parameters:

- Stepper motor step angle: 1.8 deg
- Roller screw cinematic relationship: 1mm/rev
- Diameter of the circle containing the three spherical joints centres: 424 mm

When one step is performed, the reflector rotates around the axis defined by the non translating spherical joints. The resolution is obtained by means of the trigonometric relationship between the displacement of the moving spherical joint vertical for one step and its distance to the rotation axes:

$$\text{resolution} = \sqrt{2}\arcsin\left(\frac{1.8\,\text{deg}\times\frac{1\text{rev}}{360\,\text{deg}}\times\frac{1\text{mm}}{1\text{rev}}}{424\,\text{mm}\times\cos(45\,\text{deg})}\right) = 1.35\cdot10^{-3}\,\text{deg}\ .$$

RTM accuracy is driven by the following parameters:

- Stepper motor positioning inaccuracy under a external load: 0.9 degrees (half step)
- Roller screw positioning accuracy: 0.006 mm
- Differential thermal expansion between fixed support and linear actuator: $\Delta T = \pm 60ºC$
- Diameter of the circle containing the three spherical joints centres: 424 mm

The difference between the weighed coefficient of thermal expansion between the fixed support and the linear actuator is caused by materials dissimilarity. This circumstance only happens due to the presence of stainless steel ball bearings in the actuators (the rest is titanium for both). The ball bearings as well are encased in titanium parts, so an intermediate coefficient of thermal expansion will be used. The fixed support is all titanium. Taking into account the ball bearing height (20 mm), the differential expansion will be:

$$\Delta l = 20\text{mm}\cdot\left(\frac{\alpha_{Ti}+\alpha_{SS}}{2}-\alpha_{Ti}\right)\cdot 60°\text{C} = 0.00132\text{mm}$$

For each trimming axis, the accuracy is defined as the maximum output angle error w.r.t the theoretical positioning. Taking into account the relationship between vertical displacement and output angle and considering that the combination of errors in the two axes yields a maximum of $\sqrt{2}$ axis error:

$$\text{accuracy} = \sqrt{2}\arcsin\left(\frac{0.9\,\text{deg}\times{}^{1\text{rev}}\!/_{360\,\text{deg}}\times 1\text{mm/1rev}+0.00132\,\text{mm}+0.006\text{mm}}{424\text{mm}\cdot\cos(45\,\text{deg})}\right) = 2.65\cdot10^{-3}\,\text{deg}$$

The stiffness values of the RTM in-orbit configuration, considers an antenna reflector with the following characteristics,

Parameter	Value
Antenna reflector dimensions	
diameter	12 m
mass	70 kg
main inertia	1350 kgm^2

and the resulting RTM stiffness values are,

Parameter	Value
Stiffness launch	>140 Hz
in-orbit (RTM + LDR)	> 2,5 Hz

The mechanical and thermal environments at which this RTM is qualified are the following,

Parameter	Value
Sine vibration (5 – 100 Hz)	15g (max)
Random vibration (5 – 2000 Hz)	17 grms
Operational temperatures	-40°C <-> +80°C
Non-operational temperatures	-70°C <-> +90°C

RTM mass is lower than 5 kg
The RTM interface to LDR is through three attaching areas located in a 424 mm diameter circumference. Each area consist in 6 holes for M6 bolts distributed in a 60 mm bolt pattern.
The RTM interface to ADB is through four attaching areas located in a 424 mm diameter circumference. Each area consist in 6 or 7 M4 or M6 bolts distributed in a bolt pattern.

2. NECESSITY OF A TRIMMING MECHANISM

2.1 Positioning efficiency

Parabolic reflectors are based on the geometric properties of paraboloids. When a ray coming from the focus of the paraboloid is reflected at the paraboloid, its output direction is parallel to the axis of the paraboloid. Furthermore, the total length of the ray path from the focus to a plane normal to the axis of the paraboloid is the same for every ray (FA'A = FB'B).

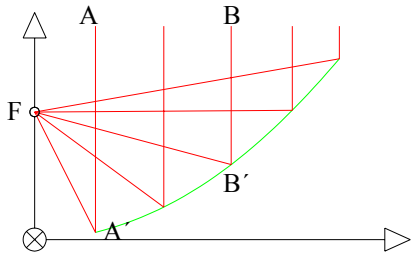

Figure 3: Parabola properties

These properties applied to RF signals make parabolic reflectors concentrate and amplify these signals. The gain (G) achieved by using a parabolic reflector depends on the RF signal wavelength (λ) and on the aperture diameter of the reflector (D):

$$G = 9.87 \cdot \left(\frac{D}{\lambda}\right)^2$$

However, this theoretical gain can never be achieved due to imperfections. The real reflecting surface does not exactly fit any paraboloid with focus at the feed and axis parallel to the direction to where the earth is (earth axis). This fact happens for the following reasons:

- Reflector surface intrinsic inaccuracy.
- Positioning accuracy, which are basically caused by spacecraft misalignments w.r.t. the earth and by thermal gradients in the arm.

To measure these "geometric" losses, it is necessary to define a magnitude, the RMS deviation; which is the root mean square deviation of the reflecting surface w.r.t. the best fit paraboloid (BFP).The BFP is the paraboloid with focus at the feed and axis parallel to the earth axis that minimizes this deviation. The geometric efficiency of a reflecting surface depends on this RMS deviation (σ) and on the wavelength of the RF signal:

$$\eta = e^{-\left(\frac{4\cdot\pi\cdot\sigma}{\lambda}\right)^2}$$

Reflector surface intrinsic inaccuracy is permanent and does not depend on the positioning of the reflecting surface w.r.t. both the feed and the earth. In order to distinguish between the efficiency loss caused by intrinsic inaccuracies and the loss caused by positioning errors, the positioning RMS deviation (σ_p) will be calculated using the nominal BFP as the reflecting surface. By doing this, the total RMS deviation (σ) is related to the intrinsic RMS deviation (σ_i) and to the positioning RMS deviation (σ_p) by the following expression:

$$\sigma^2 = \sigma_i^{\,2} + \sigma_p^{\,2} \Rightarrow \sigma = \sqrt{\sigma_i^{\,2} + \sigma_p^{\,2}}$$

Introducing this value in the efficiency formula, the resulting efficiency can be split in an intrinsic efficiency and a positioning efficiency:

$$\eta = e^{-\left(\frac{4\pi\sigma}{\lambda}\right)^2} = e^{-\left(\frac{4\pi\sigma_i}{\lambda}\right)^2 - \left(\frac{4\pi\sigma_p}{\lambda}\right)^2} = e^{-\left(\frac{4\pi\sigma_i}{\lambda}\right)^2} \cdot e^{-\left(\frac{4\pi\sigma_p}{\lambda}\right)^2} = \eta_i \cdot \eta_p$$

2.2 Spacecraft misalignments

Spacecraft misalignments imply a rotation of the nominal BFP around the feed (the relative position between feed and nominal BFP is not altered). Therefore, the rotated nominal BFP axis is not parallel to the earth axis any more so efficiency decreases. The RMS deviation of the rotated nominal BFP w.r.t. the BFP with focus at the feed and axis parallel to the earth axis is the RMS deviation caused by spacecraft misalignments.

Therefore, spacecraft misalignment RMS deviations depend exclusively on the misalignment and on the geometry of the reflector. SENER has developed a mathematical model that calculates this deviation as a function of the nominal BFP and the misalignment. In our particular case the RMS deviation for different spacecraft misalignments is shown in the following chart.

S/C misalignment (°)	0.05	0.10	0.15	0.20	0.25
RMS deviation (mm)	1.7	3.3	5.0	6.6	8.3

Table1:RMS deviations due to spacecraft misalignments

2.3 Thermal distortions

Thermal effects in the arm produce relative movement (rotation and displacement) between the feed and the reflecting surface. This movement of the reflecting surface can be described as a rotation around a thermal rotation axis. The difficulty lays on the evaluation of the different thermal cases.

SENER has assumed a case where there is a constant thermal gradient in the arm that provokes a constant torque causing a constant curvature in it. As it can be seen the axis of thermal rotations appears near the arm elbow.

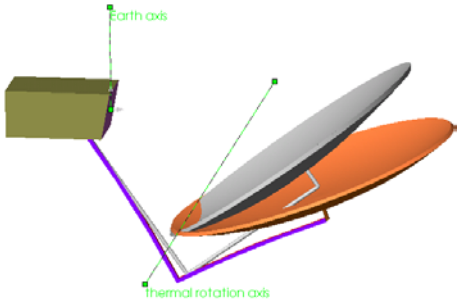

Figure 4: Assumed thermal distortion

The RMS deviation of the rotated nominal BFP w.r.t to the BFP with focus at the feed and axis parallel to the earth axis is the value to be calculated. The same mathematical model but changing the centre of rotation from the feed to the thermal rotation centre (which has been predicted for the mentioned case) shows the RMS deviation for given thermal distortions.

Thermal misalignment (degrees)	0.05	0.10	0.15	0.20	0.25
RMS deviation (mm)	2.5	5.1	7.6	10.1	12.7

Table 2: RMS deviations due to thermal misalignments

2.4 Combined effects

When both effects appear simultaneously, the total RMS deviation is the algebraic sum of partial deviations. For example a 0.1 degree spacecraft misalignment (3.3 mm RMS) combined with a 0.05 degree thermal distortion (2.5 mm RMS) causes a total deviation of 5.8 mm RMS. In the following chart the trimming efficiency for different RMS deviations when the reflector works at L-band and S-band is shown:

RMS deviation (mm)	2	4	6	8	10
Efficiency in L-band (1660 MHz) values %	98.1	92.6	84	73.4	61.7
Efficiency in S-band (2200 MHz) values %	96.7	87.3	73.7	58.1	42.8

Table 3: Loss of efficiency due to RMS deviation

For the above-mentioned case, the efficiency in S-band would be 75.2%. Rotating the reflector 0.087±0.005 degrees in the opposite direction by means of a trimming mechanism can improve up to 99.8 %.

3. DETAILED DESIGN

For description, the RTM has been divided into the following subassemblies:

1. Two linear actuator devices
2. Two torsion stiffeners
3. Three spherical joint assemblies
4. A fixed support

3.1 Linear actuator

The two linear actuators are the most complex subassemblies in the RTM. Their function is to give the linear force and displacement. They deform the sheets and overcome the external loads by transforming the rotary motion and torque of a stepper motor with a screw-nut type element. Each of them comprises the following elements :

Stepper motor

The stepper motor is the electrical device that provides the required torque to turn the roller screw.

A hybrid stepper motor of 200 steps per revolution allows a fine resolution and high torque capability. The rotor has a permanent magnet and two toothed stacks (50 teeth each). The stator has four toothed pole pairs with redundant windings in order to guarantee the required reliability. They are directly assembled to the specific shaft and housing required for RTM interfaces.

Figure 5: Stator and rotor assemblies

Roller screw

The roller screw is basically an assembly that transforms the rotation of the shaft, which is axially fixed, into an axial displacement of the nut, which is rotationally fixed. The main difference with respect to an acme screw is the efficiency. In an acme screw the relative movement implies sliding surfaces and, therefore, important friction and wear. In a roller screw the relative movement is based on rolling surfaces and, therefore, reduced friction and wear.

From the two available types of roller screws: recirculating rollers and planetary rollers, the first one has been selected as baseline since it is more suitable for high stiffness and precision applications.

The roller screw consists of a double piece nut (preloaded configuration), several threaded rollers and a spindle.

In order to guarantee the required axial stiffness and no backlash, the roller screw is preloaded by means of using a split nut and a spacer. This preload plays, as well, a very important role in order to avoid backdriving when subjected to an external axial load, which is the second function of the roller screw. The preload causes an internal friction torque, practically independent from the applied external axial load that compensates the mechanical torque caused by the applied axial load. This “irreversibility” feature is valid up to the axial load value where the mechanical torque equalizes the friction torque value.

The mechanical advantage of the roller screw depends on its lead size. In order to reduce motorization requirements and meet resolution and accuracy requirements, a 1 mm lead has been selected.

One of the ends of the roller screw shaft has a female thread to attach the flexible gimbal. The other one, serves as the end stop for both limits of the stroke (see figure 9). It consists of an increased diameter that prevents itself from getting into the roller screw nut and from getting into the end-stop that fixes the spherical joint to the linear actuator.

Axial decoupling device.

The axial decoupling device is a subsystem that decouples the top part of the linear actuator from the bottom part so they can have a relative movement, only in launch condition, and transfer low forces to the actuator, and its interfaces.

The decoupling system consists of three parts: a cylinder (with three radially flexible sheets), a piston (with three latching fingers) and a spring. The spring is encased inside the cylinder and around the piston. Due to the elasticity of the spring, the axial relative displacement between cylinder and piston is allowed in the unlatched configuration.

Figure 6, Stepper motor showing the piston of the decoupling system

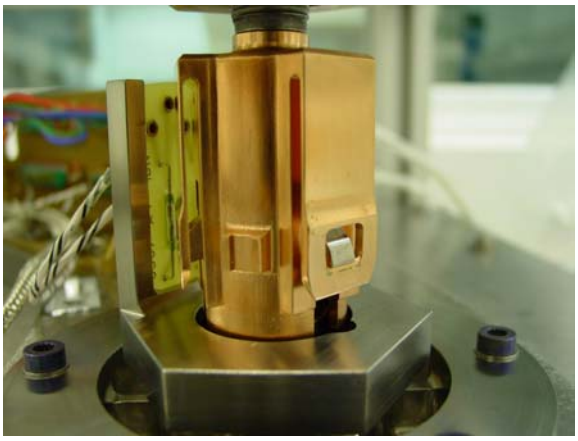

Figure 7, Axial decoupling device.

The spring compressive force provides the required preload to avoid stiffness loss under operational conditions. This self locking device needs a manual operation to unlatch (only necessary during testing).

Ball bearings

The ball bearing package consists of two angular contact ball bearings, mounted back to back in O configuration. They drive all the reactions, except the torsion, to the ADB interface. This function is necessary to mechanically decouple the stepper motor from loads that could affect its performance. The ball bearings are preloaded to provide the required stiffness eliminating backlash as well.

The inner bearing races are encased between the flexible gimbal and the motor shaft. On the other hand, the outer races are encased between the stepper motor frame. To get the adequate preload properties in the ball bearings, the flexible gimbal pushes the inner rings of the bearings against the rotor shaft.

Reed switches

To monitor that the latching of the linear decoupling device is optimally performed we have implemented a simple sensing system in the linear actuator. It consists of two reed switches (for redundancy), attached to the cover of the ball bearing package, that are electrically closed when any of the three magnets joined to the cylinder of the linear decoupling device is close enough to the switch (see figure 7).

3.2 Torsion stiffener

The main function of this subassembly is to provide the required torsion stiffness to the RTM. This is achieved by constraining the theoretical direction of the linear actuator in the torsion mode. However, in order to allow the linear actuator motion, that linear displacement needs to be allowed. These characteristics are accomplished by the selected “supported sheet structure”. It consists of a stiffness controlled “vertical” support, a “vertically” deformable “horizontal” sheet and fixing plates.

This structure provides controlled lateral stiffness to the assembly. It is connected to the ADB interface by means of a bolted flange. From this flange two triangular section columns protrude. On its two top flat surfaces the support has screw provisions for the sheet attachment.

Two deformable sheets provide the vertical elasticity to accomplish the required trimming range. They are one millimetre thickness, INVAR or aluminium sheets, very stiff longitudinally. Due to the high non-linear behaviour of the sheets caused by the stiffness controlled support constrain, the required force to deform them is significant and so it is the reaction in the support. These effects are minimised by using long sheets and providing the minimum required lateral stiffness to the dedicated support.

The sheets are made of INVAR material which is the adequate material for interfaces made of carbon fibber. If the interfaces material is aluminium, the sheets should be also made of aluminium. The change of material form INVAR to aluminium (7075, for example) would be perfectly possible.

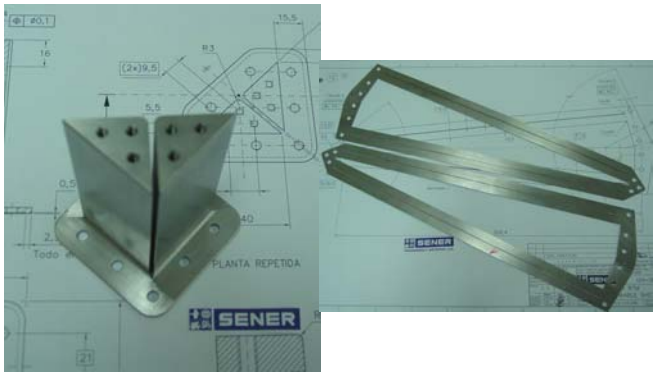

Figure 8, Torsion support structure and deformable INVAR sheets.

3.3 Three spherical joint assemblies

These three assemblies decouple the rotation of the LDR interface w.r.t the linear actuators and the fixed support, as required in order to guarantee the mechanism cinematic compatibility. Since these assemblies are in the direct stiffness path of the RTM, they need to have a high linear stiffness in both radial and axial directions.
Each assembly consists of a spherical bearing, a housing, a spherical joint cover and an end-stop cover. The inner shaft that fits into the ball is not considered part of the spherical joint assembly since they are different for the linear actuator and for the fixed support. Both the outer and inner races of the spherical joint need to be preloaded against their fittings by means of the covers to guarantee the required axial stiffness. A radial stiffness loss is avoided by means of appropriate fitting tolerances.

3.4 Fixed support

This structural part connects the ADB interface with the central spherical joint assembly. Its design is basically driven by stiffness and strength requirements, taking into account its attachment with the ADB interface and with the spherical joint assembly.
It is rigidly connected with the ADB by means of a bolted flange. The connection with the spherical joint consists of a fitting shaft ending in a external screw thread, fixed with the correspondent end-stop cover. Due to the selected interfaces, the mass optimised shape for this element is conical.

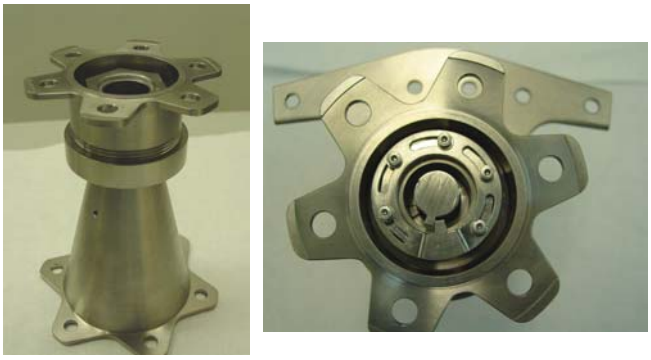

Figure 9, Fixed support structure and spherical bearing showing roller screw end-stop

4. RTM CRITICAL ANALYSES

RTM structural and thermal analyses have been performed in close cooperation with Alenia Spacio to assure the relation with System analyses at Large Deployable Antenna level.

The cooperation has been specially important to :

- Study the necessity of RTM compensation of the dynamic disturbances due to the elasticity of the system when excited by the S/C AOCS.
- Define the main RTM requirements : pointing range, torsional stiffness, launch loads…
- Find a solution for launch scenario through the axial decoupling device.
- Study the implications at system level of the latching operation. This operation has been checked successfully during the test campaign for different stiffness at the interface. The result is that it is a very well controlled operation via stepper motor.
- Simulate the trimming operation dynamically to check the reflector “delay” taking into account LDA characteristics.
- Establish an iterative philosophy for thermal analyses. At the beginning of the project, SENER performed a preliminary thermal analysis of the RTM in orbit conditions in order to define the operational temperatures of the main parts of the RTM. Once defined the RTM design, SENER provides ALS with a simple model which cover RTM geometrical definition and thermal characteristics. With this information System level analyses were performed to define the different mission scenarios.
- Analyse the sheets non-linear behaviour .

5. VERIFICATION / TEST CAMPAIGN

The critical components of the linear actuator (stepper motor, roller screw and ball bearings) were submitted to test at item level once mounted on their respectives

housing and preloaded, that means in the same final conditions than working in the mechanism.
Roller screw friction torque has been measured in the whole range of operation and in worst conditions.

Figure 10, Roller screw friction torque measurement

The RTM has being submitted to an exhaustive test campaign including, functional tests in ambient, vibration, thermal vacuum cycling and life test, according to the test sequence shown in Figure 11.

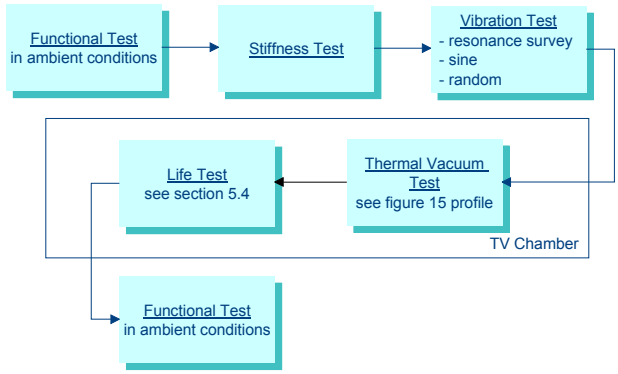

Figure 11, Test sequence

The following paragraphs describe the most outstanding results of this test campaign.

5.1 Functional

The functional test has been performed to prove the RTM capability to :

- Perform the latching process of both actuators for different stiffness in LDR and ADB interfaces.
- Test the RTM resolution and accuracy within the whole range of motion.
- Prove the RTM capability of no-backdriving.

The RTM performances are evaluated through three positioning sensors controlled by an electronic box for testing. The same equipment has been used in thermal vacuum and life test to allow results comparison.

Figure 12, Functional test

5.2 Vibrations

The vibration testing of the RTM included sine & random excitation apart from the resonance survey for eigenfrequency determination.

- Frequency survey

The frequency survey of the mechanism revealed a first natural frequency in launch configuration over 270 Hz.

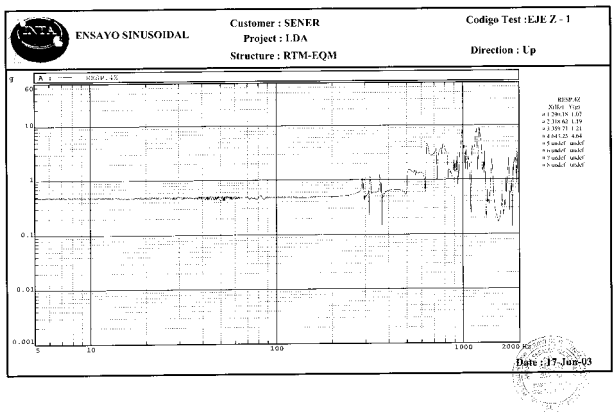

Figure 13, RTM resonance survey plot.

- Sine & random

The sine vibration test was undertaken successfully at the required levels without any notching. No relevant amplification was found due to the absence of resonances in the frequency range of the test with the exception of the INVAR sheets which amplify at their eigenfrequency. The non-linear behaviour of the sheets (increase of the stiffness when deformed) allows their survival during high level sinus (15 g´s in vertical direction) .
The random vibration test was run from 0 to 2000 Hz without any notching.

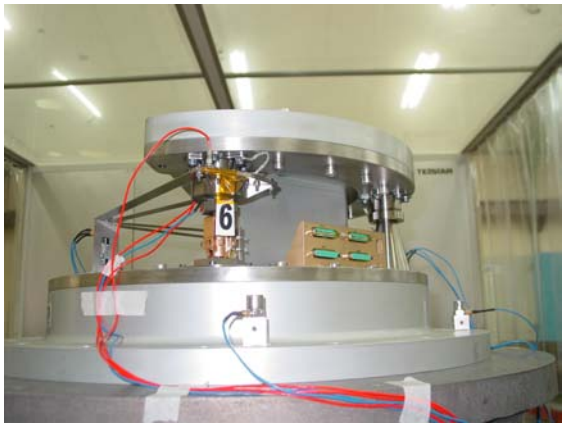

Figure 14, RTM during vibration.

5.3 Thermal cycling

The test is now runing according to the specified test profile consisting in one complete cycle between the maximum and minimum non-operating temperatures, eight complete cycles between the maximum and minimum operating temperatures and functional tests at maximum and minimum operating temperatures (including latching).

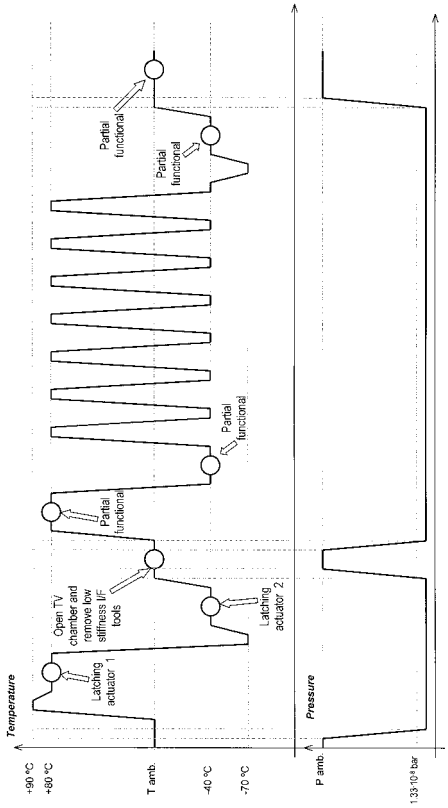

Figure 15, Thermal cycling test profile.

The thermal cycling test will demonstrate the capacity of the mechanism to survive and operate in the thermal environment expected in whole LDA mission. Latching at worst conditions and first cycle have been already performed.

5.4 Life test

The RTM EQM will be submitted to a life test in order to check the mechanisms performance after the required number of cycles .
One cycle is intended as the capability of the RTM to recover pointing errors maintaining its performances. The next table defines the three kind of cycles as required in the specification. The number of cycles has been calculated considering 2 cycles/day when eclipse occurs (25% of the days) and 1 cycle/day in the rest of the days.

	degrees	rev/cycle		n° cycles
small recovery	0,05	0,28	20%	3230
medium	0,2	1,13	70%	11303
full recovery	1,5	8,50	10%	1615

All the cycles will be performed with the same actuator (number 1) in order to check the RTM life in the worst case.
Figure 16 shows the RTM in the TV chamber .

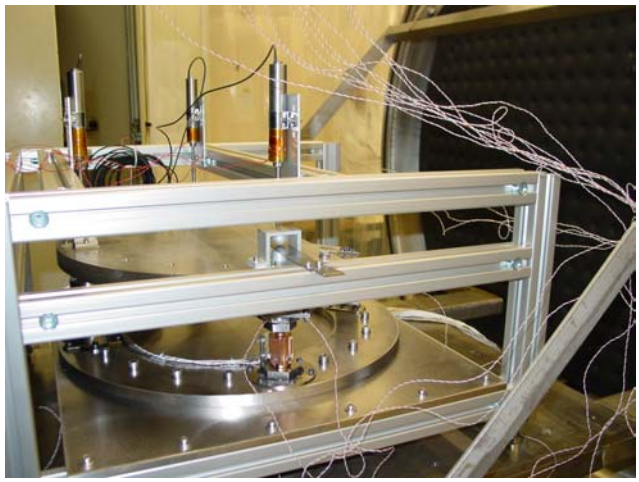

Figure 16, RTM in the TV chamber

6. CONCLUSIONS

The RTM is under SENER development (Test Readiness Review, May 2003) and will be totally qualified by September 2003.
All the pieces and components used in the RTM qualification model are flight standard. The mechanism has been submitted to an exhaustive test campaign showing that it is ready for flying.
The design is modular and allows its implementation in different reflector types and dimensions changing the distance between movable and fixed points and the lateral stiffener. The conceptual design is very competitive for high torsional stiffness.
The RTM has been designed to be operated with the same electronic box developed for moving the Antenna pointing Mechanism in Hispasat 1-C.

Back to Contents